

- t = time from release
- t_d = duration of a fireball as an effective source of thermal radiation
- t_g = time at transition between control of dispersion by momentum effects to control by gravitational effects
- t_L = fireball lift off time
- t^1 = time required for mean concentration in cloud to drop to lower flammability limit
- α = momentum of release due to flash evaporation, per unit mass
- ρ_A = density of air

REFERENCES

1. 30.4.1981, Hansard, HMSO, 432
2. Roberts, A. F., to be published
3. Hardee, H. C., and Lee, D. O., 1975, *Accid. Anal. and Prev.* 7 91-102
4. Maurer, B., Hess, K., Giesbrecht, H., and Leuckel, W., 1977, 2nd Int. Symp. on Loss Prevention, EFCE, Heidelberg, 305-321
5. Jagger, S.F., and Kaiser, G.D., 1980, 11th NATO/CCMS ITM on Air Pollution Modelling and its Applications, Amsterdam
6. Hasegawa, K., and Sato, K., 1977, 2nd Int. Symp. on Loss Prevention, EFCE, Heidelberg, 297-304
7. "Guide for pressure relief and depressurising systems" 1969, American Petroleum Institute RP-521
8. Fletcher, B., "Sudden discharge of a superheated fluid to atmosphere" This symposium
9. Stoll, A.M., and Chianta, M.A., 1971, *Trans. N.Y. Acad. of Sci., Series 2* 33 649-670
10. Gray, W.A., 1979, *Fire Prevention Science and Technology* 22 9-15
11. Lees, F.P., 1980, *Loss Prevention in The Process Industries*, Butterworth, London
12. J. Eyre., Personal communication

THERMAL RADIATION HAZARD FROM FIREBALLS

D A Lihou* and J K Maund*

Small scale fireballs were made by igniting elevated hemispherical detergent bubbles filled with butane and with natural gas, in the range 100 to 800 ml. Surface temperatures were measured by two-colour pyrometry from colour cine films of the fireballs. Fireball diameter increases at a constant rate during combustion; both diameter and elevation are dependent on the cube root of the mass of flammable gas. The ranges at which people will be severely burnt from unconfined vapour cloud fireballs and BLEVES are correlated with mass of flammable to the 0.4 power.

INTRODUCTION

Fireballs are clouds of burning gas or vapour, frequently elevated, which emit intense thermal radiation over considerable ranges. A vapour cloud which is enriched above the upper flammable limit will not explode; upon reaching a source of ignition, flame will spread around the periphery where there is enough air to dilute the vapour and bring it within the flammable range.

Shortly after ignition, the hot combustion shell will be sufficiently buoyant to cause the fireball to rise; thereby increasing the range of hazardous radiation. Air enters the fireball due to its thermally expanding shell and its rise. Thus the size and elevation of fireballs will increase during combustion and the fireball becomes extinct by breaking up into smaller pockets of gas, some of which may still be burning. Soot is produced during combustion of hydrocarbon fireballs, causing luminous flames with an emissivity of unity. Soot is produced also when natural gas clouds ignite to form fireballs; but the flames are not totally luminous and the average emissivity of the fireball surface will be less than unity.

Boiling Liquid Expanding Vapour Explosions (BLEVES) which occur when a liquefied flammable gas container bursts as a result of being engulfed in fire, produce aerial fireballs; but the initial cloud contains a significant burden of aerosol droplets so that the tendency to produce soot is increased.

*Department of Chemical Engineering, University of Aston in Birmingham.

The bursting tank produces shock waves and the work of Maurer et al (1) indicates that up to 28% of the vessel contents can be sufficiently well-mixed with air to undergo percussive deflagration.

Hazards from Fireballs

Fireballs are hazardous because they are very hot, may be very large and move in the atmosphere on currents of air. They are, therefore, sources of ignition and may ignite any combustible material in their path, but more serious is their potential effect on people who can suffer severe burns from thermal radiation even some distance away from the fireball. The disaster on the Spanish camp site (2) in 1978 in which many people were killed and injured occurred when a cloud of propene escaped from a tanker and became a fireball when it found a source of ignition. A Dutch eyewitness, interviewed by BBC Television reporters, described a cloud of white vapour rolling down over the campsite, which ignited and produced a fireball similar to a mini atomic bomb.

People were severely burnt by thermal radiation even some distance from the fireball because they were scantily clad. From the work of Stoll and Chianta (3) on the thermal radiation damage to pig skin, the following relationship has been derived. It enables the steady incident flux density \bar{q}_2 kW/m² to be related to the duration t_e seconds which will cause severe blistering.

$$\bar{q}_2 = 50/t_e^{0.71} \dots\dots\dots (1)$$

For steady radiant flux, secondary fires in buildings can occur when the flux density is 12.6 kW/m² or more (4). Process plants and flammable storage tanks suffer severe damage at 37.8 kW/m². As a general rule of thumb, one may assume that under these quoted flux densities (4), buildings and process equipment will ignite after 1000 seconds (about 17 minutes). Thus the radiation dosage for secondary fires may be set as follows:

For buildings: $\int_0^{t_e} q_2 dt = 12.6 (MJ/m^2) \dots\dots\dots (2)$

For process equipment: $\int_0^{t_e} q_2 dt = 37.8 (MJ/m^2) \dots\dots\dots (3)$

Predictions from Previous Work

With the exception of Hasegawa and Sato (5) who measured maximum incident flux densities at a point 15m from experimental BLEVES, none of the published work quotes fireball temperature nor emitted flux density. Correlations for the duration of combustion and equivalent spherical diameter of the fireball, as illustrated in equations 4 and 5, have been proposed and/or deduced from small-scale experiments. Although, not all

authors have used SI units, the parameters quoted in Tables 1 and 2 are for a mass m (kg) of flammable producing a fireball of diameter D_s (m) diameter for a duration of t_c (s).

$$t_c = A m^a \dots\dots\dots (4)$$

$$D_s = B m^b \dots\dots\dots (5)$$

TABLE 1 - Values of the Parameters in Equations 4 and 5 found Experimentally.

Flammable	Scale	A	a	B	b	Authors	Note
Methane	0.1-10kg	2.57	1/6	6.36	0.325	Hardee et al (6)	1
Propane	0.037-0.37g	2.53	1/6	6.28	1/3	Fay and Lewis (7)	2
Pentane	0.3-6.2kg	1.10	0.10	5.28	0.277	Hasegawa (5)	3
Propene	0.124-452kg	0.32	1/3	3.51	1/3	Maurer et al (1)	4
Propellants	1-10 ⁵ kg	0.49	0.320	6.20	0.320	High (9)	5

Note 1. Time elapsed before lift-off quoted as follows for methane.

$$t_1 = 1.11 m^{1/6} \dots\dots\dots (6)$$

Note 2. Soap bubbles enclosed the propane before ignition, in a method similar to that used by the present authors. The height of the top of the fireball at extinction was correlated, from which the diameter correlation has been deducted to obtain the final elevation of the bottom of the fireball.

$$H_e = 4.1m^{1/3} \dots\dots\dots (7)$$

Note 3. From BLEVES of glass vessels. The area of the fireball, viewed from the side, was plotted versus time and the duration correlated is that for which the area exceeded half its maximum value. Incident radiation at 15m range was correlated as follows:

$$q_2 = 3.1m^{0.661} \dots\dots\dots (8)$$

Note 4. The theoretical analysis of BLEVES of steel tanks has been extended by Lihou (8) to show that the constants A and B depend upon $(44.8/M)^{1/3}$. The molecular weight $M = 42$ for propene has been used to give the values quoted in Table 1; see also equations 53 and 54.

Note 5. High based his correlations on the total mass of fuel plus oxidant. Values of A and B are based upon the mass of kerosene in a stoichiometric mixture with oxygen (13).

TABLE 2 - Values of the Parameters in Equations 4 and 5 proposed in various Review Papers

Authors	Gayle (10)	Brasie (11)	Marshall (12)	Roberts (13)
A	0.245	0.30	0.38	0.45
a	0.356	1/3	1/3	1/3
B	3.68	3.8	5.5	5.8
b	0.326	1/3	1/3	1/3

Predictions from the Present Work

The emitted flux density q_1 (kW/m²) from the surface of a fireball is dependent upon the fourth power of its absolute temperature T_s (K). The principal feature of the present work is the determination of surface temperatures by two-colour pyrometry, using optically calibrated cine films. The theoretical basis of this technique is described later; the relationship between q_1 and the hazardous incident flux is presented here.

$$q_1 = \epsilon \sigma T_s^4 \dots\dots\dots (9)$$

Let F_{12} be the fraction of radiation emitted from the fireball which would shine directly on a target at a specified range. If the areas of the fireball and the target are A_1 and A_2 , respectively, the relationship between the two flux densities is as follows.

$$A_1 q_1 F_{12} = A_2 q_2 \dots\dots\dots (10)$$

Applying the reciprocity law ($A_1 F_{12} = A_2 F_{21}$) to equation 10 and allowing for attenuation by the atmosphere yields the following expression.

$$q_2/q_1 = \tau F_{21} \dots\dots\dots (11)$$

The attenuation constant for the atmosphere can vary from 0.4km⁻¹ for a clear day (visibility 10km) up to 1.0km⁻¹ for a hazy day (visibility 4km). An average value of 0.7km⁻¹ has been assumed in equation 12, in which L(m) is the distance from the edge of the fireball to the target area.

$$\tau = \exp(-7 \times 10^{-4}L) \dots\dots\dots (12)$$

For a spherical fireball of diameter D_s (m), which has cleared the ground by a height of H (m), the value of F_{21} for a target at a radial distance R (m) from a point directly below the centre of the fireball, is given by equation 13 which has been used to prepare Table 15.

$$F_{21} = \frac{(H/D_s + 0.5)}{4 \{(H/D_s + 0.5)^2 + (R/D_s)^2\}^{3/2}} \dots\dots\dots (13)$$

$$L/D_s = \{(H/D_s + 0.5)^2 + (R/D_s)^2\}^{1/2} - 0.5 \dots\dots\dots (14)$$

Table 15 shows that for targets at ranges up to about 0.75 D_s from the centre-line of the fireball, the incident flux density will decrease as the fireball rises. However, at longer ranges the flux density will increase to a maximum and then decrease as the fireball rises.

Prediction of Hazard Ranges. From an appropriate correlation, the duration of combustion can be used in equations 1, 2 and 3 to obtain limiting values of q_2 . Equation 9 gives q_1 and Table 15 is used to find the value of R/D_s for which F_{21} is approximately equal to the limiting values of q_2/q_1 in the range of $0 < H/D_s < H_e/D_s$. Equation 14 is used to calculate L from which the transmissivity is found by equation 12. Hazard ranges are found by multiplying the predicted fireball diameter D_s (m) by the limiting values of R/D_s and by the appropriate value of τ . Typically, allowance for attenuation will reduce the hazard ranges by up to 20%. Worked examples are given later, to illustrate this predictive method.

EXPERIMENTAL WORK

One way of assessing large-scale phenomena on a small and controlled scale is by modelling. The work described here generated and recorded small-scale fireballs on colour cine films. Because the density of a gas cloud determines its behaviour in the atmosphere, particularly before ignition, it was decided to investigate natural gas (methane) which has a molecular weight just more than half that of air, and Calorgas (butane) which is twice as dense as air.

Production of Gas Clouds

The apparatus used to produce undiluted flammable clouds of known volume is illustrated in Figure I. With valve V2 shut and valve V1 open, the flammable gas was admitted to the inverted cylinder C1 which was immersed in water in cylinder C2. When C1 contained sufficient gas, V1 was closed and the end of the 25mm diameter nozzle N was immersed in a 10% aqueous solution of Alkyl Ether Sulphate detergent, made by Applied Chemicals of Coventry. Valve V2 was opened and C1 was lowered in C2 to produce a gas bubble of known volume.

When studying elevated clouds, a hemispherical bubble was blown onto a wire mesh G, which was 200mm above the base of the fireball chamber. For ground clouds, the bubble was blown onto a sheet of PTFE on the floor of the fireball chamber. The walls of the chamber were lined with black paper. A grid of white lines was drawn on the rear wall.

Ignition and Measurement of Fireballs

The ignition source was a candle on a metre rule. The gas bubble was burst either by the candle flame or by a sharp wire, extending 50mm ahead of the candle, which was moved at about 20cm/s towards the side of the bubble. For elevated clouds burst by ignition, the candle was raised under the centre of the bubble.

Time, Elevation and Size Measurement. A 16mm cine film was exposed at 64 frames per second of the fireballs, in semi-darkness so as to be self-illuminating against the black background. The white scale markings were illuminated by two photoflood lamps, shown as P in Figure I. The film contained also a large-dial clock which rotated once every 2 seconds. This showed that the camera accelerated to its set speed within 5 frames and remained at constant speed. Time was measured by counting the number of frames after ignition was observed.

When the film was projected, the projector was adjusted relative to the screen to obtain an integer value of the scale, typically 1/5th full size. The elevation of the bottom of the fireball from the mesh G or from the ground was measured from the projected film, which was analysed one frame at a time. Immediately after ignition, the butane gas clouds slumped through the mesh before becoming buoyant; negative elevations were recorded during this interval.

Examination of early films showed that a few fireballs were roughly spherical; but most fireballs ranged from prolate to oblate spheroids and some were mushroom shaped. The latter were assumed to be oblate spheroids surmounting a cylinder. In order to estimate the volume of the fireballs for the mathematical models, it was decided to convert all the measurements to "equivalent spherical diameters", representing the diameter of a sphere having the same volume as the fireball.

For this it is only necessary to measure the depth and width of the luminous image, to note whether the shape was approximately cylindrical, spheroidal (rounded corners) or mushroom shaped, and to assume that the plan shape was circular, all reasonable measurements and assumptions. Then, for vertical cylinders of image width (diameter) w and depth h , the equivalent spherical diameter D_s is:

$$D_s = (1.5 w^2 h)^{1/3} \dots \dots \dots (15)$$

and for the spheroidal shapes:

$$D_s = (w^2 h)^{1/3} \dots \dots \dots (16)$$

Temperature Measurement. The only method of temperature measurement, that does not rely on heat transfer to the sensor, depends on measuring colour temperature of an incandescent source. The higher the temperature of the source, the bluer the light it emits.

The light intensity at a given wavelength λ_1 is given by Wien's law:

$$I_{\lambda_1} = A (\lambda_1)^{-5} \epsilon_{\lambda_1} \exp (- B/\lambda_1 T) \dots \dots \dots (17)$$

where:

I_{λ_1} = light intensity at wavelength λ_1 (lux)
 ϵ_{λ_1} = emissivity at wavelength λ_1
 T = temperature of source (K)
 A, B are constants.

Figure II illustrates this relationship, showing the relative intensities at different wavelengths (colours) of sunlight (mean surface temperature of sun = 6000K) and a 100 watt tungsten filament lamp (mean filament temperature = 2800K).

It is difficult to use Wien's law directly for temperature measurement, although it has been done (14), because while the wavelength of measurement λ_1 may be known, the values of the constants A and B and the emissivity ϵ are not; the light intensity depends not only on the temperature but also on the amount of gas burning. However, by taking the Wien's law equations for two wavelengths (λ_1 and λ_2) and dividing them by each other, the comparative form is obtained:

$$\frac{I_{\lambda_1}}{I_{\lambda_2}} = \left\{ \frac{\lambda_2}{\lambda_1} \right\}^5 \frac{\epsilon_{\lambda_1}}{\epsilon_{\lambda_2}} \exp \left[\frac{B}{T} \left\{ \frac{1}{\lambda_2} - \frac{1}{\lambda_1} \right\} \right] \dots \dots \dots (18)$$

For luminous flames Lyn (15) found that emissivity was practically constant with wavelength, therefore $\epsilon_{\lambda_1}/\epsilon_{\lambda_2} = 1$.

Taking natural logarithms of equation 18 gives

$$\ln \left\{ \frac{I_{\lambda_1}}{I_{\lambda_2}} \right\} = 5 \ln \left\{ \frac{\lambda_2}{\lambda_1} \right\} + \frac{B}{T} \left\{ \frac{1}{\lambda_2} - \frac{1}{\lambda_1} \right\}$$

$$\ln \left\{ \frac{I_{\lambda_1}}{I_{\lambda_2}} \right\} = K_1 + \frac{K_2}{T} \dots \dots \dots (19)$$

Where K_1 is only a function of the two wavelengths chosen.

Schack (16) has demonstrated that carbon particles in a luminous flame exhibit grey body radiation and that their temperature is within 1K of the true flame temperature, so that measurement of light intensities emitted by incandescent carbon particles in a flame at two known wavelengths should be a sound method of measuring the flame temperature. Maund (17) successfully used optical filters with a fairly narrow bandwidth for temperature measurements of the combustion process inside an operating diesel engine, so it was decided to use photographic filters of known wavelength transmission

properties for this work. In order to avoid overlap, filters in the red and blue regions of the visible spectrum were chosen. Kodak Wratten filters No. 47 (blue) and No. 29 (red) were used and their transmission characteristics are presented in Figure III. These filters are designed for colour separation work and have characteristic wavelengths of 630nm (red) and 450nm (blue).

For his diesel engine studies, Maund (17) placed a glass window in the wall of the combustion chamber, focussed and split the emerging beam of light into two halves and passed the two resulting beams through photographic filters to two photomultipliers connected to a synchronised double-beam oscilloscope. This technique is not possible for fireballs because they vary in size and shape and they move, so that it

is not possible to focus the light from them on to suitable detectors. However, since the fireballs were being filmed for size measurement the idea was conceived of photographing them in colour and then analysing the resulting permanent film record for red and blue intensity and, therefore, temperature. Colour reversal film has three emulsions, sensitive to red, green and blue light; the red and blue sensitivities correspond closely to the wavelengths of the chosen filters - see Figure IV. Kodak VNF (Video News Film) was chosen because of its rapid processing.

In order to allow for the many variables which affect the colour balance of the developed film, two luminous flames of known temperature were included in every frame of the films. The standard flames were of methane and butane; shown as M and B respectively, in Figure I. The value of K_1 in equation 19 is known from the characteristic wavelengths of the Wratten filters. The known temperatures of the standard flames enabled two checks to be made of the constancy of K_2 in equation 19.

The temperature of the surface of the non-aerated calibration flames was measured by scanning the flames using a very fine wire thermocouple, near the surface, and extrapolating the resulting curve to the surface position - Figure V. The surface temperature of the methane flame was 1236K and that of butane was 1275K.

The remaining device needed was a photosensitive detector with a known intensity/output characteristic, sensitive to both red and blue light. A cadmium sulphide photoresistor (type ORP12) was chosen since this has a very wide logarithmic response to light intensity (Figure VI) and resistance is simple to measure. The device also has reasonable sensitivity to all wavelengths of visible light. The photocell was mounted at the end of a short blackened tube so that light from a particular spot on the film could be projected on to it, through the appropriate filter in turn, without it being affected by stray light from other parts of the picture. The projection arrangements are illustrated in Figure VII.

On each frame, the temperature of the brightest surface zone was recorded as the maximum temperature. Then the projector lens was adjusted to give a defocussed image of uniform colour. The light intensities from this image gave the average surface temperature.

Experiments Completed

Two series of experiments have been carried out by students (18, 19) as part of their MSc course. In the first series, butane-filled bubbles were either allowed to fall onto the candle or were ignited while hanging from the nozzle. The cine films were not calibrated for two-colour pyrometry in the first series of experiments; but fireball size, elevation and duration were correlated empirically with mass of butane, which ranged from 1.5g to 6g.

In the second series (19), methane and butane fireballs were made and analysed as described above. Elevated and ground level clouds were burst by ignition and before ignition. Volumes ranged from 100ml to 800ml, corresponding to 0.24g to 1.9g for butane and 0.07g to 0.6g for methane. Empirical correlations with mass of flammable were found for maximum spherical diameter, maximum elevation and duration of the visible fireballs.

Accuracy

Measurements of fireball dimensions and elevation from the projected films were accurate to $\pm 10\%$. Calculation of equivalent spherical diameter would have errors ranging from $\pm 10\%$ for uniform shapes to $\pm 20\%$ for the more irregularly shaped fireballs.

Values of K_2 were calculated from the two calibration flames on a frame of the film just before ignition and on a frame after the fireball was extinct. These four values of K_2 were always within $\pm 5\%$ of their mean. Over 30m of cine film the values of K_2 were within $\pm 10\%$ of their mean. Accuracy of temperature measurements is within $\pm 20K$.

EXPERIMENTAL RESULTS

The results reported here are for elevated clouds burst by the ignition source. These show the changes at 0.05 second intervals of the size, elevation and temperature of the fireballs. Figure VIII shows these data plotted for a 400ml (0.972g) fireball, indicating the closeness of fit of the mathematical models which are presented in the following section. Other data are tabulated here and should be compared with the predicted data summarised in Tables 12, 13 and 14.

Analysis of the cine films of ground level clouds and of elevated clouds burst before ignition has not yet been carried out frame by frame; but observations near the end of combustion has enabled empirical correlations, with mass of flammable gas, to be proposed for maximum elevation and the duration of combustion to these maxima (18, 19).

TABLE 3 - Experimental Data for 100ml Elevated Butane Cloud - Burst by Ignition

Time s	Max. Temp. K	Av. Temp. K	Width m	Depth m	Diam. m	Elevation m
.05	1290	1375	.085	.174	.108	-.084
.10	1318	1235	.160	.155	.158	-.060
.14	1312	1236	.175	.240	.194	-.040
.20	1362	1282	.180	.260	.233	-.020
.25	1394	1271	.265	.400	.304	0
.31	1401	1308	.340	.510	.360	.010
.36	1383	1300	.425	.625	.449	.030
.41	1412	1297	.460	.625	.480	.060
.45	1362	1300	.400	.560	.447	.175
.50	1317	1255	.475	.325	.419	.550
.55	1145	1134	.525	.365	.465	.550
.60	1037	1098	.550	.300	.449	.675
.64	1026	1260	.525	.225	.396	.750
.69	-	-	.550	.125	.336	.800

Mass = 2.43×10^{-4} kg. Temperature Calibration $K_2 = 2700K$.

TABLE 4 - Experimental Data for 200ml Elevated Butane Cloud - Burst by Ignition

Time s	Max. Temp. K	Av. Temp. K	Width m	Depth m	Diam. m	Elevation m
.05	1234	1368	.130	.130	.130	0
.10	1264	1404	.165	.150	.160	0
.15	1296	1213	.300	.150	.238	0
.20	1218	1260	.310	.200	.268	0
.25	1287	1257	.350	.275	.323	.005
.30	1312	1250	.350	.375	.358	.010
.35	1285	1220	.375	.425	.391	.025
.40	1369	1278	.475	.500	.483	.035
.45	1337	1303	.550	.425	.505	.125
.50	1304	1264	.600	.425	.535	.275
.55	1372	1305	.640	.465	.575	.300

Mass = 4.86×10^{-4} kg. Temperature Calibration $K_2 = 2612K$.
This fireball divided into two after 0.6 seconds, the larger part was extinguished at 0.95s at a height of 1.1m; the smaller part lasted to 0.8s at a height of 0.875m.

TABLE 5 - Experimental Data for 300ml Elevated Butane Cloud - Burst by Ignition

Time s	Max. Temp. K	Av Temp K	Width m	Depth m	Diam. m	Elevation m
.05	-	-	.160	.100	.136	-.05
.10	1208	1308	.275	.125	.211	-.05
.15	1234	1195	.300	.240	.278	-.05
.20	1214	1178	.350	.260	.317	-.04
.25	1315	1222	.400	.325	.373	-.03
.30	1309	1232	.425	.400	.416	-.02
.35	1261	1235	.450	.450	.450	0
.40	1299	1247	.525	.550	.533	.025
.45	1295	1219	.600	.600	.600	.075
.50	1258	1180	.600	.625	.608	.110
.55	1244	1223	.600	.600	.600	.175
.60	1240	1202	.600	.600	.600	.225
.65	1177	1133	.700	.650	.683	.300
.70	1050	1041	.675	.600	.649	.500
.75	-	1196	-	-	-	.750

Mass = 7.29×10^{-4} kg. Temperature Calibration $K_2 = 2434K$.

TABLE 6 - Experimental Data for 500ml Elevated Butane Cloud - Burst by Ignition

Time s	Max. Temp. K	Av Temp K	Width m	Depth m	Diam. m	Elevation m
.05	1310	2029	.085	.220	.134	-.120
.10	1356	1117	.165	.280	.196	-.120
.15	1391	1364	.290	.225	.266	-.100
.20	1261	1260	.360	.285	.333	-.090
.25	1358	1270	.400	.340	.379	-.060
.30	1349	1259	.380	.410	.390	-.030
.35	1362	1293	.360	.465	.448	-.010
.39	1288	1280	.350	.510	.454	0
.45	1334	1293	.450	.635	.577	.050
.50	1393	1307	.525	.575	.600	.100
.55	1380	1336	.600	.450	.624	.325
.60	1344	1231	.700	.525	.636	.375
.65	1408	1236	.700	.550	.646	.400
.70	1279	1181	.700	.515	.632	.525
.75	1219	1081	.750	.510	.660	.575
.80	1074	1014	.825	.500	.698	.600
.85	1000	1033	.875	.450	.701	.775
.90	1012	1003	.900	.500	.740	.825

Mass = 12.15×10^{-4} kg. Temperature Calibration $K_2 = 2723K$.

TABLE 7 - Experimental Data for 600ml Elevated Butane Cloud - Burst by Ignition

Time s	Max. Temp. K	Av. Temp. K	Width m	Depth m	Diam. m	Elevation m
.05	-	-	.125	.175	.160	-.100
.11	1256	1214	.250	.175	.222	-.100
.15	-	-	.325	.250	.298	-.100
.20	1345	1208	.350	.290	.329	-.090
.25	-	-	.350	.350	.350	-.080
.30	1222	1256	.425	.400	.416	-.050
.35	-	-	.500	.500	.500	-.020
.39	1377	1280	.575	.575	.575	0
.45	-	-	.600	.650	.616	.150
.50	1333	1282	.625	.550	.600	.160
.55	-	-	.675	.590	.645	.225
.60	1357	1285	.750	.575	.686	.325
.65	-	-	.775	.650	.731	.390
.70	1312	1217	.800	.675	.756	.450
.75	1128	1148	.800	.750	.783	.450
.80	1032	1036	.800	.750	.783	.550
.84	1061	1023	.850	.750	.815	.600
.89	1086	990	.850	.700	.797	.725
.94	1026	1035	.800	.800	.800	.750

Mass = 14.58×10^{-4} kg. Temperature Calibration $K_2 = 2680K$.

TABLE 8 - Experimental Data for 200ml Elevated Methane Cloud - Burst by Ignition

Time s	Max. Temp. K	Av. Temp. K	ϵ	Width m	Depth m	Diam. m	Elevation m
.05	-	-	0.1	.150	.075	.119	.005
.10	1380	1472	0.4	.175	.130	.158	.020
.15	1320	1375	0.3	.225	.175	.207	.050
.20	1618	1499	0.6	.250	.225	.241	.075
.25	1405	1417	0.8	.280	.250	.270	.090
.30	1383	1346	0.8	.325	.240	.294	.125
.35	1257	1256	0.7	.325	.275	.307	.150
.40	1714	1790	0.5	.375	.200	.304	.200
.45	-	-	0.3	.350	.200	.290	.250

Mass = 1.34×10^{-4} kg. Temperature Calibration $K_2 = 2187K$.
 ϵ = Estimated proportion of fireball surface which was luminous.

TABLE 9 - Experimental Data for 400ml Elevated Methane Cloud-Burst by Ignition

Time s	Max. Temp. K	Av. Temp. K	ϵ	Width m	Depth m	Diam. m	Elevation m
.05	-	-	0.3	.200	.100	.159	.005
.10	1262	1452	0.4	.240	.230	.237	.010
.15	1345	1479	0.6	.300	.300	.300	.015
.20	1286	1441	0.6	.350	.350	.350	.090
.25	1263	1360	0.8	.325	.390	.345	.120
.30	1377	1273	0.9	.360	.390	.370	.150
.35	1249	1282	0.9	.380	.375	.378	.340
.40	1310	1388	0.9	.430	.380	.413	.415
.45	1272	1319	0.7	.450	.400	.433	.460
.50	1259	1350	0.3	.530	.440	.498	.500
.55	1297	1344	0.15	.590	.380	.510	.585
.60	1392	1680	0.4	.340	.220	.294	.675

Mass = 2.68×10^{-4} kg. Temperature Calibration $K_2 = 2149K$.
 ϵ = Estimated proportion of fireball surface which was luminous.

TABLE 10 - Experimental Data for 600ml Elevated Methane Cloud-Burst by Ignition

Time s	Max. Temp. K	Av. Temp. K	ϵ	Width m	Depth m	Diam. m	Elevation m
.05	-	-	0	.050	.105	.064	.005
.10	-	-	0	.200	.125	.171	.010
.15	-	-	0	.250	.165	.218	.030
.20	-	-	0	.335	.300	.323	.050
.25	1440	-	0.2	.360	.350	.357	.075
.30	1584	-	0.5	.395	.400	.397	.100
.35	1398	1408	0.9	.375	.450	.398	.125
.40	1260	1295	1.0	.450	.450	.450	.200
.45	1254	1306	1.0	.450	.375	.423	.350
.50	1236	1316	1.0	.510	.400	.470	.400
.55	1308	1502	1.0	.550	.300	.548	.600
.60	1517	2035	0.6	.615	.360	.514	.600
.65	-	-	0.1	.900	.325	.641	.700

Mass = 4.02×10^{-4} kg. Temperature Calibration $K_2 = 2104K$.
 ϵ = Estimated proportion of fireball surface which was luminous.

TABLE 11 - Experimental Data for 800ml Elevated Methane Cloud-Burst by Ignition

Time s	Max.Temp. K	Av.Temp. K	Width m	Depth m	Diam. m	Elevation m
.05	1791	1928	.125	.090	.112	.010
.10	-	-	.225	.250	.233	.030
.15	-	-	.340	.325	.335	.050
.20	-	-	.325	.300	.316	.100
.25	-	-	.450	.350	.414	.225
.30	1980	-	.475	.375	.439	.250
.35	1765	-	.500	.360	.448	.300
.40	1450	-	.550	.375	.591	.330
.45	1596	-	.640	.390	.543	.410
.50	1494	-	.670	.410	.569	.475
.55	-	-	.720	.430	.606	.540
.60	-	-	.750	.400	.608	.600
.65	-	-	.650	.400	.553	.700

Mass = 5.35×10^{-4} kg. Temperature Calibration $K_2 = 2060K$. There was negligible luminosity on the surface of this fireball, which made it difficult to measure meaningful temperatures. Being the largest possible volume for elevated clouds with the detergent solution used, the bubble may have burst just before ignition allowing premixing of air.

MATHEMATICAL MODELS

Two models based upon material and heat balances have been developed, which fit the observed diameter and elapsed time relationships. Both models are based upon the experimental observation that the diameter of fireballs increased at a constant rate.

The model described as a Hot Shell - Cold Core fits the experimental data from this work. The duration of combustion in these small-scale experiments is an order of magnitude longer than is predicted for large-scale fireballs; although the diameters after combustion is complete are comparable. Therefore, it is postulated that large fireballs are sufficiently turbulent to produce an isothermal, homogeneous fireball; this model is called the Isothermal model.

Hot Shell - Cold Core Model

In this model the core of the fireball is at ambient temperature, which for the experiments was 290K. Prior to neutral buoyancy, for the butane fireballs, the core is assumed to contain no air. But when the fireballs begin to rise air enters the core without being heated. Air required for combustion is consumed at the hot shell.

Pre-lift off Combustion of Butane. The butane cloud is initially at 290K, so the following heat balance can be written:

$$m h \frac{df}{dt} = mrc (T_s - 290) \frac{df}{dt} + \pi D^2 \sigma \epsilon T_s^4 \dots (20)$$

m is the mass of flammable originally in the cloud, of which a fraction f burns in time t, with a net calorific value h.r is the mass ratio of combustion products from the stoichiometric combustion of unit mass of the flammable gas; these products have a mean specific heat C. The hot shell, with an equivalent spherical diameter D, has a temperature T_s and emissivity ϵ ; while σ is the Stefan-Boltzmann constant.

It has been noted that throughout combustion, the equivalent spherical diameter increases at a constant rate $(dD/dt)_c$. Rearranging the above equation and cancelling dt by making the substitution:

$$D^2 dt = D^2 dD (dt/dD)_c \dots (21)$$

enables the integration to be carried out, with the boundary conditions $f = 0$ when $D = D_0$; where

$$D_0 = 3.57 (m/M)^{1/3} \dots (22)$$

and M is the molecular weight of the flammable gas.

$$f = \frac{\pi \epsilon \sigma T_s^4 (D^3 - D_0^3)}{3m\{h - rC(T_s - 290)\} (dD/dt)_c} \dots (23)$$

At neutral buoyancy the fireball density equals that of the surrounding air which at 290K with a mean molecular weight of 29 has a density of 273/224 kg/m³. Let $f = f_1$ and $D = D_1$ at lift-off; the fireball mass is $m(1 + rf_1)$ and its volume is $\pi D_1^3/6$. Equating its density to 273/224 and rearranging gives

$$D_1^3 = 1.567 (1 + rf_1) m \dots (24)$$

Substituting f_1 and D_1^3 in equation 23 and substituting $\sigma = 56.7 \times 10^{-12} \text{ kW/m}^2$ gives the following general equation for denser-than-air gases.

$$f_1 = \frac{93.05 \epsilon (T_s/1000)^4 (1 + rf_1 - 29/M)}{\{h - rC(T_s - 290)\} (dD/dt)_c} \dots (25)$$

For butane: $r = 17.14$, $C = 1.14 \text{ kJ/kg K}$, $M = 58$, $h = 45920 \text{ kJ/kg}$ and from the experiments the following mean values were found: $T_s = 1300\text{K}$, $\epsilon = 1$, $(dD/dt)_c = 1 \text{ m/s}$. Substituting these values in equation 25 gives $f_1 = .00614$.

From equations 22 and 24, and putting $(dD/dt)_c = 1$ gives the following relationships for butane:

$$D_0 = 0.92 \text{ m}^{1/3} \dots (26)$$

$$D_1 = 1.20 \text{ m}^{1/3} \dots (27)$$

$$t_1 = 0.28 \text{ m}^{1/3} \dots (28)$$

Dilution and Combustion. During the completion of combustion of butane clouds, and throughout the combustion of methane clouds, air at 290K enters the core at an average radial velocity \bar{U} m/s through the hot shell. \bar{M} is the average molecular weight of a stoichiometric mixture of combustion products. The rate of increase of volume can be expressed as follows:

$$\frac{\pi D^2}{2} \left(\frac{dD}{dt} \right)_c = \frac{\pi r}{M} * \frac{22.4}{273} (T_s - 290) \frac{df}{dt} + \pi D^2 \bar{U} \dots (29)$$

The heat balance shown as equation 20 still applies, because the excess air enters the core without being heated. Combining equations 20 and 29 gives the following heat and mass balance relationship.

$$m h \frac{df}{dt} = \pi D^2 \left[\sigma \epsilon T_s^4 + \frac{273 \bar{M} C}{22.4} \left\{ 0.5 \left(\frac{dD}{dt} \right)_c - \bar{U} \right\} \right] \dots (30)$$

For butane, the boundary conditions are $f = f_1$, $D = D_1$, which is given by equation 24. This equation can be used to eliminate m , having made the substitution shown as equation 21 and integrating.

$$f = f_1 + \frac{448(1 + rf_1)}{273h(dD/dt)_c} \left\{ \left(\frac{D}{D_1} \right)^3 - 1 \right\} * Q \dots (31)$$

$$Q = \sigma \epsilon T_s^4 + \frac{273 \bar{M} C}{22.4} \left\{ 0.5 \left(\frac{dD}{dt} \right)_c - \bar{U} \right\} \dots (32)$$

Let $D = D_c$ at the completion of combustion when $f = 1$. The experimental data for butane is best fitted by putting $\bar{U} = 0.5 (dD/dt)_c$, which eliminates the second term in equation 32. Additional constants for butane are $M = 28.4$, $f_1 = 0.00614$ and $D_1 = 1.2 \text{ m}^{1/3}$. Substitution in equation 31 gives

$$D_c = 6.45 \text{ m}^{1/3} \dots (33)$$

Since $t_c = (D_c - D_0)/(dD/dt)_c$ and for methane $(dD/dt)_c = 1 \text{ m/s}$ we get the following expression for the duration of the combustion phase.

$$t_c = 5.53 \text{ m}^{1/3} \dots (34)$$

For methane, the boundary conditions for equation 30 are $f = 0$ at $D = D_0$, which is found from equation 22 with $M = 16$. Other constants are: $r = 19$, $C = 1.22 \text{ kJ/kg K}$, $\bar{M} = 27.6$, $h = 50213 \text{ kJ/kg}$ and from the experiments the following mean values were found: $T_s = 1500\text{K}$, $\epsilon = 0.5$, $(dD/dt)_c = 1 \text{ m/s}$. These parameters in the following equation with $f = 1$ at $D = D_c$ and $t = t_c$, with Q given by equation 32 when $\bar{U} = 0.5 (dD/dt)_c$ produce equations 36 and 37. The duration of combustion given by equation 34.

Equations 35, 36 and 37 may be found under Table 16.

TABLE 12 - Predicted Values for Butane from the Hot Shell - Cold Core Model

Volume Mass		Pre-lift off Phase			Dilution and Combustion Phase	
ml	10 ⁻³ kg	D ₀ (m)	D ₁ (m)	t ₁ (s)	D _c (m)	t _c (s)
100	.243	.057	.075	.018	.402	.345
200	.486	.072	.094	.022	.507	.435
300	.729	.083	.108	.025	.581	.498
400	.972	.091	.119	.028	.639	.548
500	1.215	.098	.128	.030	.688	.590
600	1.458	.104	.136	.032	.731	.627

TABLE 13 - Predicted Values for Methane from the Hot-Shell - Cold Core Model during Combustion

Volume (ml)	200	400	600	800
Mass (10 ⁻³ kg)	.134	.268	.402	.536
D ₀ (m)	.073	.092	.105	.115
D _C (m)	.356	.448	.513	.565
t _C (s)	.283	.356	.408	.449

Isothermal Model

In this model the whole fireball is assumed to be burning at an isothermal temperature T_C. Combustion is controlled by the supply of air and ceases after a time t_C which is correlated empirically with the mass m of the flammable gas initially in the cloud. The equivalent spherical diameter starts at D₀ and increases at a constant rate (dD/dt)_C up to a diameter D_C at which the fuel has all disappeared. A fraction (1 - f_C) of the fuel is assumed to be cracked to produce soot, the volume of which is neglected. The final diameter D_C is found for a stoichiometric mixture of combustion products from the burnt fraction f_C of the fuel plus a fraction (1 - f_C) of residual air, all at a temperature of T_C.

The stoichiometric molar ratio of air to flammable gas is v and n is the increase in the total number of moles per mole of flammable gas burnt stoichiometrically. The volumetric rate at which air flows into the fireball is V m³/s when the equivalent spherical diameter is D. Other symbols are defined in the previous model and are listed at the end of this paper.

The rate of increase of volume can be written as follows:

$$\frac{\pi D^2}{2} \left(\frac{dD}{dt} \right)_C = \frac{VT_C}{290} (1 + nf_C/v) \dots (38)$$

$$\text{Combustion rate (kW)} = \frac{273 VMhf_C}{290 \cdot 22.4v} \dots (39)$$

$$\text{Sensible heat to air (kW)} = \frac{273 \cdot 29 \cdot VC_a (T_C - 290)}{290 \cdot 22.4} \dots (40)$$

where C_a is the specific heat of air.

$$\text{Radiative heat loss (kW)} = \pi D^2 \epsilon \sigma T_C^4 \dots (41)$$

Substitution for V from equation 38 into equations 39 and 40, writing the heat balance equation and cancelling πD² leaves the following equation after substituting σ = 56.7x10⁻¹² kW/m² and C_a = 1.09 kJ/kgK.

$$9.30 \epsilon \left(\frac{T_C}{1000} \right)^4 = \left\{ \frac{Mhf_C - 31.61v (T_C - 290)}{T_C (v + nf_C)} \right\} \left(\frac{dD}{dt} \right)_C \dots (42)$$

For a gas cloud of mass m, molecular weight M, initially at 290K, the initial and final diameters are given by equations 43 and 44.

$$D_0 = 0.539 \{290 m/M\}^{1/3} \dots (43)$$

$$D_C = 0.539 \{v + (n+1)f_C\}^{1/3} (T_C m/M)^{1/3} \dots (44)$$

The constant rate of increase of diameter is given by (D_C - D₀)/t_C where the duration of combustion is correlated empirically by equation 4, with a = 1/3. This gives the final heat and material balance equation from which the fireball temperature is related to A and f_C.

$$17.26A \epsilon \left(\frac{T_C}{1000} \right)^4 = \left[\frac{Mhf_C - 31.61v (T_C - 290)}{T_C (v + nf_C)} \right] \left[\frac{\{v + (n+1)f_C\} T_C - 290}{M} \right]^{1/3} \dots (45)$$

For butane ε = 1, h = 45920 kJ/kg, M = 58, v = 32.5, n = 1.5. The fraction of butane cracked can be estimated as the ratio of the heat of formation to the heat of combustion of butane, which gives f_C = 0.95. Taking A = 0.45, the value recommended by Roberts (13) in Table 2, gives T_C = 1993K (1720°C). Similarly, for f_C = 0.7 and A = 0.45, T_C = 1723K (1450°C).

Taking f_C = 0.95 and T_C = 1993K, equation 44 gives the following expression for the final diameter of butane fireballs, which is in good agreement with the value of B recommended by Roberts (13) in Table 2.

$$D_C = 5.72 m^{1/3} \dots (46)$$

The initial diameter D₀ is given by equation 26. The duration of combustion is given by equation 47 as follows, from which the rate of growth of diameter for large fireballs would appear to be about 10.7 m/s.

$$t_C = 0.45 m^{1/3} \dots (47)$$

For methane h = 50213 kJ/kg, M = 16, v = 10, n = 0 and ε can be set at unity to allow for soot in large fireballs. The ratio of heat of formation to heat of combustion for methane would give f_C = 0.91. Again taking A = 0.45 in equation 45 gives T_C = 1953K (1680°C). Equation 44 gives

$$D_C = 5.92 m^{1/3} \dots (48)$$

The initial diameter is given by equation 36 and t_c is given by equation 47; showing that for methane fireballs $(dD/dt)_c = 10$ m/s.

Elevation

The experiments with elevated fireballs, the results of which are reported in Tables 3 to 11, showed that the velocity of rise was very nearly equal to $(dD/dt)_c$. For butane, equations 26, 46 and 47 indicate that for large-scale fireballs $(dD/dt)_c = 10.7$ m/s. Similarly, equations 36, 47 and 48 show that for large-scale methane fireballs $(dD/dt)_c = 10$ m/s.

The time which elapses before butane fireballs become buoyant is obtained by dividing $(D_1 - D_0)$ by $(dD/dt)_c$. From equations 26 and 27 with $(dD/dt)_c = 10.7$ m/s, the correlation for the time before lift-off is as follows.

$$t_1 = 0.026m^{1/3} \dots\dots\dots (49)$$

In terms of the duration of combustion t_1 is about 6% and for the evaluating hazard ranges its effect on elevation may be neglected. Taking a rate of rise of 10m/s, the simple relationship for all large-scale fireballs is as follows.

$$H = 10t \dots\dots\dots (50)$$

The final elevation given by equation 50 is $4.5m^{1/3}$, which agrees quite well with the correlation found by Fay and Lewis (7) for propane, which is shown as equation 7.

Extinction

From the experimental results tabulated in the previous section, the duration of fireballs until the flame is extinct does not vary much over the 8-fold change of volume. These extinction times can be correlated empirically with mass of flammable gas, as shown in equations 51 and 52 and in Table 14.

$$\text{For butane: } t_e = 2.78m^{1/6} \dots\dots\dots (51)$$

$$\text{For methane: } t_e = 2.34m^{1/6} \dots\dots\dots (52)$$

The parameters given in equations 51 and 52 agree very well with those found by Fay and Lewis (7) and by Hardee et al (6), which are quoted in Table 1.

Boiling Liquid Expanding Vapour Explosions

Based upon the work of Maurer et al (1), Lihou (8) has derived the following relationships for the duration of BLEVES and the diameter of the "hot core", as described by the authors (1).

$$t_c = 0.31 \left\{ \frac{44.8 m}{M} \right\}^{1/3} \dots\dots\dots (53)$$

$$D_s = 3.44 \left\{ \frac{44.8 m}{M} \right\}^{1/3} \dots\dots\dots (54)$$

TABLE 14 - Extinction Times Predicted by Equations 51 and 52.

Volume ml	Butane		Methane	
	Mass 10 ⁻³ kg	Extinction Time(s)	Mass 10 ⁻³ kg	Extinction Time(s)
100	.243	.694	.067	.472
200	.486	.780	.134	.529
300	.729	.834	.201	.566
400	.972	.875	.268	.594
500	1.215	.908	.335	.617
600	1.458	.936	.402	.636
800	1.944	.982	.536	.667

Maurer et al (1) show that the maximum amount of LFG which will burn in the time available for mixing with air is 70%. Only about 40% of this flammable mass (that is 28% of the original contents of the vessel) has sufficient micro-mixing to undergo percussive deflagration. Thus 42% of the flammable, originally in the tank, produces a fireball.

Using equations 53 and 54 in a heat balance, based upon 42% of m undergoing isothermal stoichiometric combustion at T_c , with a constant diameter D_s , the following equation is obtained from which T_c may be found by interaction. An emissivity of unity is assumed and the symbols have the meanings used previously.

$$\frac{69700}{M} \left\{ \frac{T_c}{1000} \right\}^4 = h - 1000rC \left[\left\{ \frac{T_c}{1000} \right\} - 0.290 \right] \dots\dots (55)$$

For butane, $M = 58$, $h = 45920$ kJ/kg, $r = 17.14$ and $C = 1.14$ kJ/kg K which gives $T_c = 1880$ K. For methane, $M = 16$, $h = 50213$ kJ/kg, $r = 19$ and $C = 1.22$ kJ/kg K which gives $T_c = 1500$ K.

HAZARD RANGES

Worked examples are presented below for fireballs and BLEVES from 1000 kg of butane and methane. Hazard ranges to people for larger clouds are tabulated. Owing to the thermal inertia of buildings and process equipment, incorporated in equations 2 and 3, process equipment is unlikely to be damaged even by 100 tonne fireballs. These large fireballs will cause secondary fires in buildings which are directly under the fireball.

H/D _s	R/D _s																
	0	.25	.5	.6	.7	.8	.9	1.0	1.2	1.4	1.6	1.8	2.0	2.5	3.0		
0	1.00	.716	.354	.262	.196	.149	.115	.089	.057	.038	.027	.019	.014	.010	.0075	.0057	.0044
0.1	.694	.546	.315	.246	.191	.150	.119	.095	.062	.042	.030	.022	.016	.012	.0088	.0067	.0052
0.2	.510	.426	.275	.223	.180	.146	.118	.096	.065	.046	.033	.024	.018	.013	.0100	.0077	.0060
0.3	.391	.340	.238	.200	.166	.138	.115	.095	.067	.048	.035	.026	.020	.015	.0111	.0085	.0067
0.4	.309	.276	.206	.178	.152	.129	.109	.092	.067	.049	.036	.028	.021	.016	.0120	.0093	.0073
0.5	.250	.228	.179	.158	.137	.121	.103	.088	.066	.049	.037	.029	.022	.017	.0128	.0100	.0079
0.6	.207	.192	.156	.140	.124	.109	.096	.084	.064	.049	.038	.029	.023	.018	.0135	.0106	.0084
0.7	.174	.163	.137	.124	.112	.100	.089	.079	.061	.048	.038	.030	.024	.018	.0141	.0111	.0089
0.75	.160	.151	.128	.117	.106	.096	.086	.076	.060	.047	.037	.030	.024	.019	.0145	.0113	.0091
0.8	.148	.140	.120	.111	.101	.091	.082	.074	.059	.047	.037	.030	.024	.019	.0149	.0115	.0093
0.9	.128	.122	.106	.099	.091	.084	.076	.069	.056	.045	.036	.030	.024	.019	.0151	.0119	.0096
1.0	.111	.107	.095	.089	.083	.076	.070	.064	.053	.043	.036	.029	.024	.019	.0154	.0122	.0099
1.2	.087	.084	.076	.073	.068	.064	.060	.055	.047	.040	.033	.028	.023	.019	.0154	.0126	.0104
1.4	.069	.067	.063	.060	.057	.054	.051	.048	.042	.036	.031	.026	.023	.019	.0153	.0127	.0106
1.6	.057	.056	.052	.050	.048	.046	.044	.042	.037	.033	.029	.025	.022	.018	.0151	.0127	.0107
1.8	.047	.046	.044	.043	.041	.040	.038	.036	.033	.029	.026	.023	.020	.017	.0147	.0125	.0106
2.0	.040	.039	.038	.037	.036	.035	.033	.032	.029	.027	.024	.021	.019	.016	.0141	.0122	.0105

TABLE 15 - Direct exchange factors for spherical fireballs of diameter D_s to targets at range R_t when the fireball has cleared the ground by H

P₂₁: Incident Flux Density/Emitted Flux Density

Emitted Fluxes

Based upon the Isothermal Model, the surface temperature of methane and butane fireballs are independent of size.
 For methane T_c = 1953 K and from equation 9; q₁ = 825 kW/m².
 For butane T_c = 1993 K and equation 9 gives q₁ = 895 kW/m².

Based upon the BLEVE Model, the fireball temperatures and emitted fluxes are as follows:
 For methane T_c = 1500 K and equation 9 gives q₁ = 287 kW/m².
 For butane T_c = 1880 K and equation 9 gives q₁ = 708 kW/m².

Methane BLEVE

From equation 54: D_s = 48.49m. From equation 53: t_c = 4.37s. Substituting t_e = t_c in equation 1 gives the maximum constant flux which people can withstand, q₂ = 17.5 kW/m². Thus q₂/q₁ = .061 and with H/D_s = 0.5, Table 15 shows R/D_s = 1.26. From equation 14: L/D_s = 1.109; thus L = 53.8m. From equation 12: τ = .963 and R_h = .963 * 1.26 * 48.49 = 59m.

Butane BLEVE

Using the equations listed above for methane, the results are:

D_s = 31.56m, t_c = 2.84s, q₂ = 23.8 kW/m², q₂/q₁ = .034, R/D_s = 1.675, L/D_s = 1.45, L = 45.8m, τ = .968, R_h = 51m.

TABLE 16 - Hazards to People from BLEVES

	Butane				Methane			
	10 ³	5*10 ³	10 ⁴	5*10 ⁴	10 ³	5*10 ³	10 ⁴	5*10 ⁴
Mass of LFG (kg)	31.56	54.0	68.0	116.2	48.49	82.9	104.5	178.7
Fireball Diam. (m)	2.84	4.86	6.13	10.48	4.37	7.47	9.41	16.1
Duration (s)	23.8	16.3	13.8	9.43	17.5	12.0	10.2	6.95
Fatal Flux (kW/m ²)	.034	.023	.019	.013	.061	.042	.036	.024
Flux Ratio (q ₂ /q ₁)	1.675	1.97	2.15	2.50	1.26	1.52	1.625	1.94
Range/Diameter	45.8	82.8	116	238	53.8	91.2	125	269
Beam length (m)	.968	.944	.922	.846	.963	.938	.916	.829
Transmissivity	51	100	135	246	59	118	156	287
Hazard Range (m)								

$$f = \frac{44-8*290}{273Mh} \left(\frac{D}{D_0} \right)^3 - 1 \} * Q \dots\dots\dots (35)$$

$$D_0 = 1.42 \text{ m}^{1/3} \dots\dots\dots (36)$$

$$D_c = 6.95 \text{ m}^{1/3} \dots\dots\dots (37)$$

Fireballs

Owing to the steady increase in diameter during combustion, the incident flux q_2 at any range increases throughout. Setting t_c in equation 1 equal to the duration of combustion t_c gives the average flux \bar{q}_2 to produce fatal burns. The hazard range is the value of R at which the time - averaged integral of q_2 equals \bar{q}_2 . Let the integral at any R be called I_R .

$$I_R = \frac{1}{t_c} \int_0^{t_c} q_2 dt \dots\dots\dots (56)$$

As a first approximation, R is found for the fireball diameter and elevation, midway through the combustion. Incident flux q_2 at this range R is evaluated at 1 second intervals and these values are integrated by trapezium rule, so that the right side of equation 56 is evaluated. The correct value of the hazard range R_h is found by the inverse square law as follows:

$$R_h = R (I_R/\bar{q}_2)^{\frac{1}{2}} \dots\dots\dots (57)$$

Methane Fireball. From equation 36: $D_0 = 14.2$ m. From equation 48: $D_c = 59.2$ m. From equation 47: $t_c = 4.5$ s. From equation 1: $\bar{q}_2 = 17.2$ kW/m². Thus $q_2/q_1 = 17.2/825 = .0208$.

Midway through the combustion, $D = 36.7$ m and equation 50 gives $H = 22.5$ m. Thus $H/D = 0.6$ and from Table 15, $R/D_s = 2.11$. Neglecting atmospheric attenuation at this stage, gives the first estimate of the hazard range as 77m.

TABLE 17 - Incident Flux at 77m Range from a 10³ kg Methane Fireball at 1 Second Intervals

t(s)	D(m)	R/D	H(m)	H/D	L/D	τ	F_{21}	q_2 (kW/m ²)
1	24.2	3.18	10	.413	2.81	.954	.0063	4.96
2	34.2	2.25	20	.585	2.00	.953	.0174	13.68
3	44.2	1.74	30	.679	1.60	.952	.0317	24.90
4	54.2	1.42	40	.738	1.38	.949	.0463	36.25
4.5	59.2	1.30	45	.760	1.31	.947	.0531	41.49

At $t = 0$, $q_2 = 0$ so that using the trapezium rule to integrate equation 56 gives

$$I_{77} = \frac{4.96 + 13.68 + 24.90 + 36.25/2 + (36.25 + 41.49)/4}{4.5}$$

$$= 15.95 \text{ kW/m}^2$$

The range at which $I_R = \bar{q}_2$ is given by equation 57:

$$R_h = 77 * (15.95/17.2)^{\frac{1}{2}} = 74\text{m.}$$

Note that if atmospheric attenuation, giving $\tau = .953$, had been allowed for the initial estimate of R_h would have been 73m.

Butane Fireball. From equation 26: $D_0 = 9.2$ m. From equation 46: $D_c = 57.2$ m. From equation 47: $t_c = 4.5$ s and $\bar{q}_2 = 17.2$ kW/m² as for the methane fireball, above. Thus $q_2/q_1 = 17.2/895 = .0192$.

Midway through the combustion, $D = 33.2$ m and equation 50 gives $H = 22.5$ m. Thus $H/D = 0.68$ and from Table 15, $R/D_s = 2.2$. Estimated hazard range = 73m.

TABLE 18 - Incident Flux at 73m Range from a 10³ kg Butane Fireball at 1 Second Intervals

t(s)	D(m)	R/D	H(m)	H/D	L/D	τ	F_{21}	q_2 (kW/m ²)
1	19.9	3.67	10	.502	3.30	.955	.0045	3.85
2	30.5	2.39	20	.656	2.15	.955	.0154	13.16
3	41.2	1.77	30	.728	1.65	.953	.0307	26.19
4	51.8	1.41	40	.772	1.40	.951	.0464	39.49
4.5	57.2	1.28	45	.787	1.32	.949	.0538	45.70

From equation 56.

$$I_{73} = \frac{3.85 + 13.16 + 26.19 + 39.49/2 + (39.49 + 45.70)/4}{4.5}$$

$$= 18.72 \text{ kW/m}^2$$

$$R_h = 73 * (18.72/17.2)^{\frac{1}{2}} = 76\text{m}$$

TABLE 19 - Hazards to People from Fireballs

	Butane				Methane			
	10 ³	5x10 ³	10 ⁴	5x10 ⁴	10 ³	5x10 ³	10 ⁴	5x10 ⁴
Mass of Cloud (kg)								
Initial Diam. (m)	9.2	15.7	19.8	33.9	14.2	24.3	30.6	52.3
Final Diam. (m)	57.2	97.8	123	211	59.2	101	128	218
Final Elevation (m)	45	76.9	96.9	166	45	76.9	96.9	166
Duration (s)	4.50	7.69	9.69	16.6	4.50	7.69	9.69	16.6
Fatal Flux (kW/m ²)	17.2	11.7	9.97	6.81	17.2	11.7	9.97	6.81
Flux Ratio (\bar{q}_2/\bar{q}_1)	.019	.013	.011	.008	.021	.014	.012	.008
Transmissivity	.953	.910	.875	.780	.952	.909	.871	.771
Hazard Range (m)	76	155	201	393	74	158	208	400

Generalised Correlation

The hazard ranges listed in Tables 16 and 19 have been correlated by the following empirical formulae:

$$R_h = P m^{0.4} \dots \dots \dots (58)$$

The average values of P for each type of fireball and the ranges of values around the means are as follows:

- For Butane BLEVES: $P = 3.29 \pm 3\%$
- For Methane BLEVES: $P = 3.84 \pm 2.5\%$
- For Butane Fireballs: $P = 5.08 \pm 2.5\%$
- For Methane Fireballs: $P = 5.10 \pm 3.5\%$

DISCUSSION

The measurements summarised in Tables 3 to 11 are very satisfactorily correlated by the Hot Shell-Cold Core Model developed in this paper. Heat and material balances have been used in this model; so that the final correlations for equivalent spherical diameter and duration are fundamentally sound. See equations 26, 33, 34, 36 and 37.

Duration of Combustion

It is clear that the duration of combustion for the scale of experiments so far completed, does not scale up to fit the relationships proposed by others; although the correlation for extinction time, equation 51 and 52 agree well with Fay and Lewis (7) and Hardee et al (6), both of whom

used a similar experimental procedure. Correlations for duration of combustion, based upon the 1/3rd power of mass of flammable gas, have arisen from this experimental work because it was found that fireball diameter increases linearly with time. The 1/6th power dependence shown in equations 51 and 52 for extinction times is empirical. Fay and Lewis (7) obtained the 1/6th power relationship by incorporating a dimensionless time parameter which contained fireball volume to the 1/6th power.

Isothermal Fireball Model

Experiments with larger gas clouds need to be completed in order to validate the Isothermal Model. This model is based on the experimental observation that fireball diameter increases at a constant rate, independent of the size of flammable cloud. However, using equation 47 as an appropriate correlation for the duration of large-scale fireballs has led to fireball temperatures of 1993K for butane and 1953K for methane. These surprisingly high temperatures could have been reduced to the experimentally measure temperatures of 1275K and 1236K, respectively, by assuming about 60% of the flammable remains unburnt in the heat balance. Resolution of this conflict must await larger scale experiments.

BLEVE Fireball Model

The BLEVE fireball model which has been derived from the experimental and theoretical work of Maurer et al (1) is based upon only 42% of the contents of the vessel producing a fireball. The mechanism whereby vapour clouds are formed in BLEVES is very different to the pure unconfined vapour cloud which quickly ignites to produce a fireball. Therefore, a quasi-instantaneous fireball of constant diameter and $H/D_s = 0.5$ has been considered in formulating the model of hazard ranges to people from BLEVES.

Hazard Ranges for People

The method demonstrated in this paper, for evaluating the hazard ranges to people from fireballs which are growing and rising steadily with time, seems to be very effective. It is particularly satisfying to have been able to correlate hazard ranges for fireballs and for BLEVES with a single relationship using mass of flammable to the 0.4th power; see equation 58. If the proposed larger scale experiments demonstrate that the fireball temperatures predicted from the Isothermal Model were indeed too high, the effect will be to reduce the values of P to be used in equation 58. In the meantime, use of equation 58 with the quoted values of P is recommended, for evaluating the thermal radiation hazard ranges for the public, which may be exposed to fireballs from vapour clouds or BLEVES.

CONCLUSIONS

- * The surface temperatures of fireballs produced when neat clouds ignite are 1300 ± 20 K for butane and 1500 ± 20 K methane.
- * Equivalent spherical diameter of fireballs increases at a constant rate throughout combustion.
- * Hazard ranges at which normally clad people will suffer severe burns is correlated with mass of flammable to the 0.4th power; see equation 58.
- * The method of recording fireballs on temperature-calibrated colour cine film effectively stores a considerable amount of valuable data from a few experiments.
- * The experiments need to be repeated with vapour clouds of up to one tonne, in order to validate the effects of scale-up on: firstly the duration of combustion and secondly, through measured temperatures and a heat balance, the completeness of combustion.

SYMBOLS USED

- a = numerical exponent
- A = numerical constant
- b = numerical exponent
- B = numerical constant
- C = specific heat of combustion products (kJ/kg K)
- C_a = specific heat of air (kJ/kg K)
- D = equivalent spherical diameter of fireball (m)
- D_c = equivalent spherical diameter at completion of combustion (m)
- D₁ = equivalent spherical diameter at neutral buoyancy (m)
- D_o = equivalent spherical diameter of gas cloud (m)
- D_s = equivalent spherical diameter of hot shell (m)
- (dD/dt)_c = constant rate of increase of diameter during combustion (m/s)
- f = fraction of fuel burnt
- f_c = fraction of fuel burnt at the end of combustion
- f₁ = fraction of fuel burnt to produce neutral buoyancy
- F₁₂ = view factor from fireball to a target
- F₂₁ = view factor from target to the fireball surface
- h = net calorific value of fuel (kJ/kg)
- H = elevation of bottom of fireball above ground (m)
- H_e = elevation of fireball at extinction (m)
- IR = time-averaged incident flux density at a range of R metres (kW/m²)
- I_λ = Intensity of light at wavelength λ (lux)
- K₁ = numerical constant calculated from the wavelength transmissions of two filters
- K₂ = temperature calibration of film (K)
- L = distance from surface of fireball to target (m)
- m = mass of flammable in cloud initially (kg)
- M = molecular weight of the flammable
- M̄ = mean molecular weight of stoichiometric combustion products

- n = increase in total number of moles per mole of flammable gas burnt stoichiometrically
- P = numerical constant
- q₁ = emitted flux density from fireball surface (kW/m²)
- q₂ = incident flux density on a target area (kW/m²)
- Q₂ = average flux density to produce severe burns (kW/m²)
- Q = heat flux density function, equations 31 and 32 (kW/m²)
- r = mass ratio of combustion products per unit mass of flammable gas, from stoichiometric combustion
- R = distance radially along the ground from the centre-line of a fireball (m)
- R_h = hazard range for severe burns to people (m)
- t = time since ignition (s)
- t_c = duration of combustion (s)
- t_e = exposure time for people (s)
- t₁ = time elapsed before neutral buoyancy (s)
- T = absolute temperature (K)
- T_c = isothermal temperature of fireball (K)
- T_s = temperature of hot shell (K)
- U = average radial velocity of air through the hot shell (m/s)
- V = volumetric rate of flow of air into fireball (m³/s)
- ε = emissivity
- ε_λ = emissivity at wavelength λ
- λ = wavelength (nm)
- v = stoichiometric molar ratio of air to flammable gas
- σ = Stefan-Boltzmann constant (56.7 x 10⁻¹² kW/m²K⁴)
- τ = transmissivity of the atmosphere.

REFERENCES

1. Maurer, B., Hess, K., Giesbrecht, H., and Leukel W., 1977, "Modelling of vapour cloud dispersion and deflagration after bursting of tanks filled with liquefied gas", 2nd Int. Symposium on Loss Prevention and Safety Promotion in the Process Industries, Heidelberg, p. 305. Dechema, Frankfurt, 1978.
2. Aris, S., Dawe, A., and Brown, T., 1978, "The Los Alfraques Disaster", Sunday Times, July 16th, p. 17.
3. Stoll, A.M., and Chianta, M.A., 1971, Trans. N.Y. Acad. Sci., pp. 649-670.
4. Robertson, R.B., 1976, "Spacing in chemical plant design against loss by fire", I Chem E Symp. Ser. No. 47, p. 157.
5. Hasegawa, K., and Sato, K., 1977, "Study of the fireball following steam explosion of n-pentane", 2nd Int. Symposium on Loss Prevention and Safety Promotion in the Process Industries, Heidelberg, p. 297. Dechema, Frankfurt, 1978.
6. Hardee, H.C., Lee, D.O., and Benedick, W.B., 1978, Combustion Science and Technology, 17, 189.
7. Fay, J.A., and Lewis, D.H., 1977, "Unsteady burning of unconfined fuel vapour clouds", 16th Symposium (International) on Combustion, pp. 1397-1405. The Combustion Institute, Pittsburgh.

8. Lihou, D.A., 1981, "Hazard identification and control in the process industries", p. 50. Oyez Publishing Ltd., London.
9. High, R.W., 1968, Annals N.Y. Acad. Sci., **152**, 441-451.
10. Gayle, J.B., and Bransford, J.W., 1965, NASA Tech. Memo No. X-53314.
11. Brasie, W.C., 1976, Loss Prevention, **10**, 135. Chem. Eng. Progress Tech. Manual. AICHe, New York.
12. Marshall, V.C., 1977, The Chemical Engineer No. 323, 573. IChemE, Rugby.
13. Roberts, A.F., 1980, "Thermal radiation hazards from releases of LPG from pressurised storage", HSE, Research and Laboratory Services Division, Report No. IR/L/FR/80/20.
14. Potter, J.H. and Dillaway, R.B., 1953, Trans. ASME, **75**, 1311.
15. Lyn, W.T., 1957, J.Inst. Petr., **43**, 25.
16. Schack, F.F., 1925, Tech. Physik., **6**, 530.
17. Maund, J.K., 1959, "Combustion in diesel engines", Ph.D. Thesis, University of Birmingham.
18. Dada, M.M., 1980, "Thermal radiation from fireballs", M.Sc. Thesis, University of Aston in Birmingham.
19. Karmali, K.J., 1981, "Thermal radiation from fireballs of LPG and LNG vapour clouds", M.Sc. Thesis, University of Aston in Birmingham.

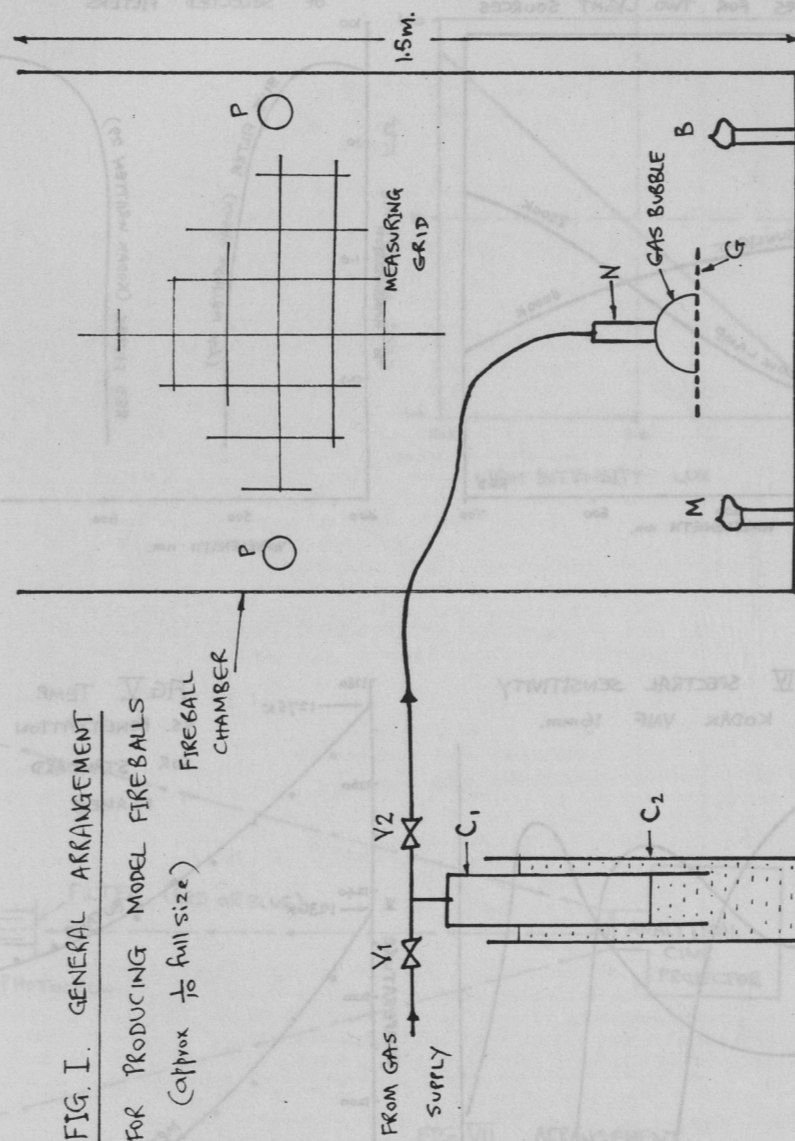


FIG. II SPECTRAL INTENSITY CURVES FOR TWO LIGHT SOURCES

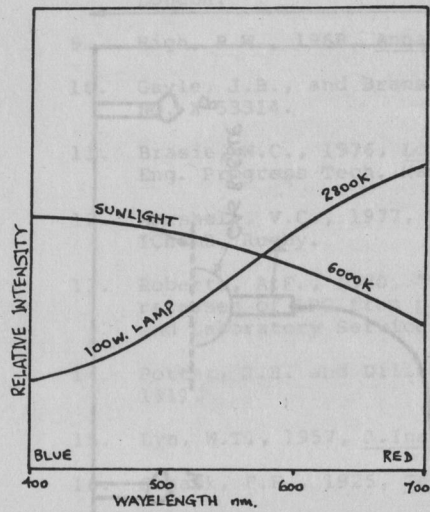


FIG. III SPECTRAL TRANSMISSION OF SELECTED FILTERS

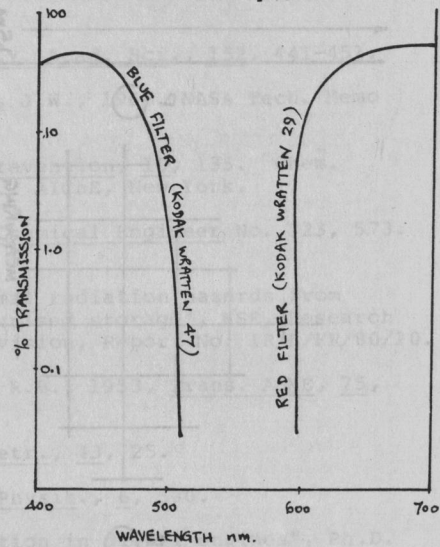


FIG. IV SPECTRAL SENSITIVITY KODAK VNF 16mm.

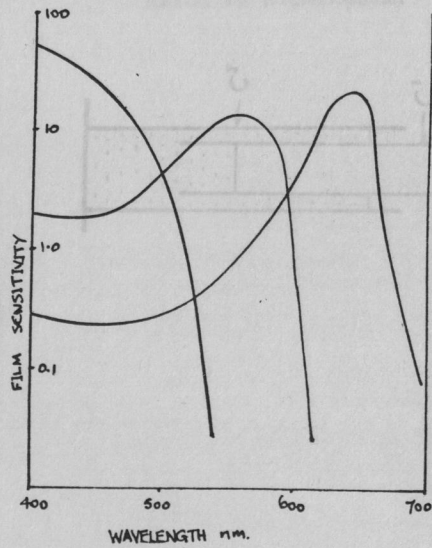


FIG. V TEMP. VS. PENETRATION FOR STANDARD FLAMES.

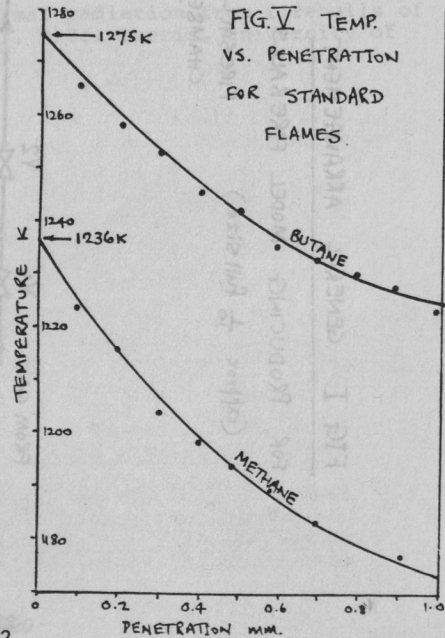


FIG. VI ORP12 PHOTOCELL CHARACTERISTIC

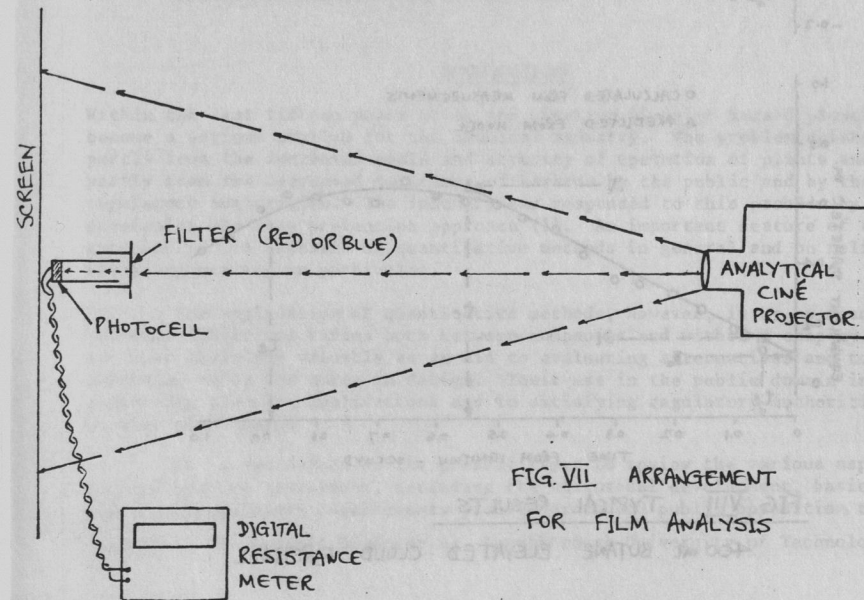
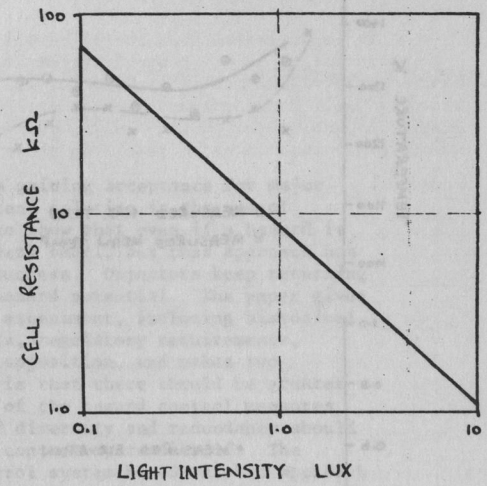


FIG. VII ARRANGEMENT FOR FILM ANALYSIS

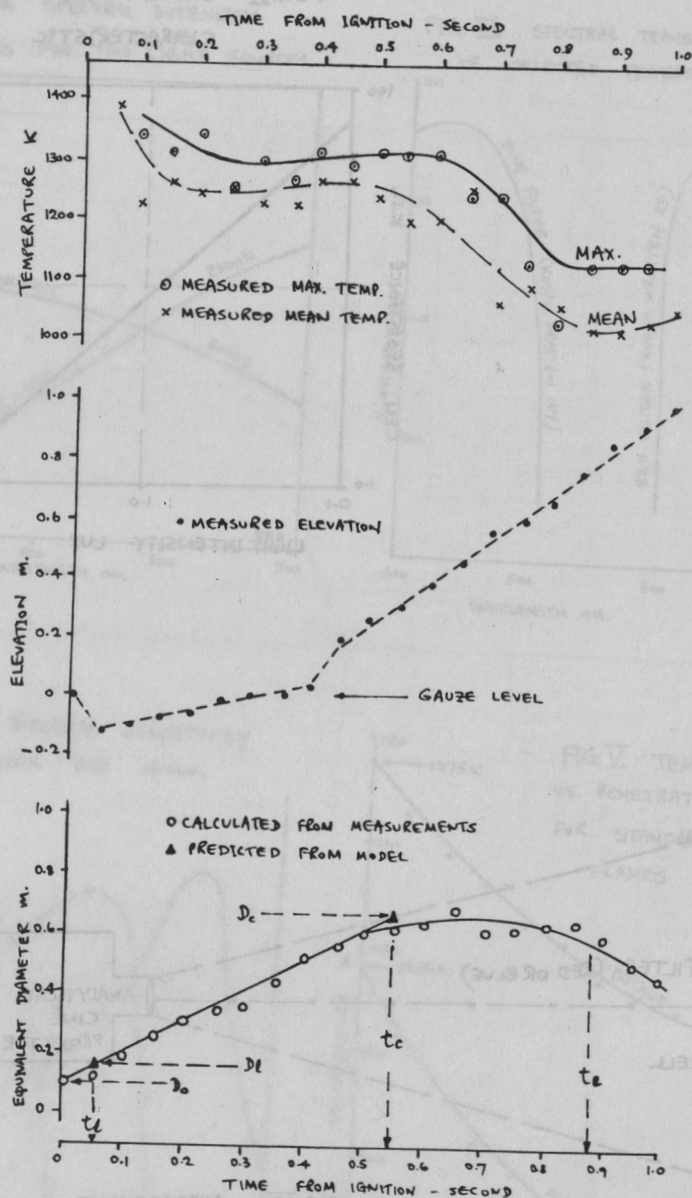


FIG. VIII TYPICAL RESULTS

400 ml. BUTANE ELEVATED CLOUD FIREBALL

QUANTITATIVE ASSESSMENT AND RELIABILITY ENGINEERING OF MAJOR HAZARD PLANTS IN THE CONTEXT OF HAZARD CONTROL

F. P. Lees*

Industry has a problem in gaining acceptance for major hazard plants. One apparent solution is the use of quantitative assessment to show that even if a hazard is very large, the risk is very small, but this approach has not been an unqualified success. Objectors keep returning to the magnitude of the hazard potential. The paper gives a review of quantitative assessment, including historical background, basic elements, regulatory requirements, problem areas and public opposition, and makes two proposals. One proposal is that there should be greater emphasis on the totality of the hazard control measures and that the principle of diversity and redundancy should be applied to the hazard control system itself. The elements of a hazard control system based on this approach are described. The other proposal is that the concept of hazard warning structure should be exploited. Most hazards have a warning structure such that there is a high probability that before the worst case accident occurs there will be a number of near misses, or warnings. The concept of hazard warning structure is described and a formal methodology, including the hazard warning tree and associated mathematics, is outlined.

INTRODUCTION

Within the last fifteen years or so the question of major hazard plants has become a serious problem for the chemical industry. The problem arises partly from the increased scale and severity of operation of plants and partly from the decreased tolerance of hazards by the public and by the regulatory authorities. The industry has responded to this problem by developing the loss prevention approach (1). An important feature of this approach is its emphasis on quantitative methods in general and on reliability engineering in particular.

The application of quantitative methods, however, is by no means uniform. Their use varies both between companies and within a company. They are most obviously valuable as an aid to evaluating alternatives and to obtaining value for money in design. Their use in the public domain in supporting planning applications and in satisfying regulatory authorities is more problematic.

It is the object of the present paper to review the various aspects of quantitative assessment, including the historical development, basic elements, regulatory requirements, problem areas and public opposition, to

* Department of Chemical Engineering, Loughborough University of Technology